Nanoscale

Highly Conductive, Pliable and Foldable Cu/Cellulose Paper Electrode Enabled by Controlled Deposition of Copper Nanoparticles

Journal:	*Nanoscale*
Manuscript ID	NR-COM-09-2018-007123.R2
Article Type:	Paper
Date Submitted by the Author:	22-Nov-2018
Complete List of Authors:	Yang, Yang; South China University of Technology, Huang, Quanbo; South China University of Technology Payne, Gregory; University of Maryland Biotechnology Institute, Center for Biosystems Research Sun, Run-Cang; Dalian Polytechnic University Wang, Xiaohui; South China University of Technology

Journal Name

ARTICLE

Highly Conductive, Pliable and Foldable Cu/Cellulose Paper Electrode Enabled by Controlled Deposition of Copper Nanoparticles

Received 00th January 20xx,
Accepted 00th January 20xx

DOI: 10.1039/x0xx00000x

www.rsc.org/

Yang Yang, [a] Quanbo Huang,[a] Gregory F. Payne, [b] Runcang Sun [c] and Xiaohui Wang*[a]

There is great interest in extending cellulosic platforms to applications in flexible, lightweight, low-cost and sustainable electronics. The critical need is the development of methods to confer electronic properties to these materials platforms (i.e., paper and fabrics). Here we report a highly conductive, pliable and foldable Cu/Cellulose paper electrode enabled by a simple low-cost and scalable wet-processing method to coat a Cu nanoparticles (NPs) layer on common cellulose paper, where polydopamine adhesion and electroless deposition were used to yield highly conductive paper with a sheet resistance as low as 0.01 Ω/sq. This Cu/cellulose paper has excellent stability because of the strong adhesion between Cu NPs and cellulose, and because the methods are sufficiently mild to prevent damage to the paper substrate. This fabrication method results in the controlled deposition of Cu NPs and yields Cu/cellulose paper with highly hydrophobic and self-cleaning properties, high photothermal conversion efficiency, excellent electromagnetic interface (EMI) shielding effectiveness. This high-performance Cu/cellulose paper could have promising application potential for a range of emerging applications in flexible electronics and packaging.

Introduction

There are exciting opportunities for flexible electronics for applications that include sensors, actuators, batteries, displays, circuits, solar cells, electronic skin, and implantable medical devices, yet these emerging applications will require electronic materials with high conductivities and pliabilities. Plastic materials such as polyethylene terephthalate (PET), polyethersulfone (PES),[1] and polyethylene naphthalate (PEN)[2] have emerged as the first-generation of substrate materials for a wide range of flexible electronics and greatly advanced the development of this area. However, there are still some limitations to plastic substrates. For example, most plastics have high coefficient of thermal expansion (CTE), which would induce large shape change during thermal processing. More importantly, the non-renewability, low biocompatibility and potential toxicity of plastic materials are affecting their applications in bio-related fields and adding burden to the environment.[3] This latter concern is becoming more and more urgent with the rapid development of consumer electronics leading to large amounts of electronic waste.[4, 5]

Alternately, widely accessible bio-based materials such as cellulose paper with good biocompatibility, biodegradability, flexibility and foldability have recently attracted great attention for future green and disposable flexible electronics.[5-8] Cellulose is thermally stable with more than an order of magnitude lower CTE than plastics, most metals, and ceramics, which is important to maintain the dimensional stability under thermal processing conditions.[9] Cellulose paper also has excellent mechanical properties and printability, it can be adapted to high-speed roll-to-roll printing, and it can be folded by common methods to form complex 3D structures (e.g., by paper origami and kirigami).[10, 11] For example, paper folding and cutting techniques are used to: increase the energy density of lithium-ion batteries;[12] enhance the efficiency of solar cells;[13] or develop deformable photodetector arrays.[14] More intriguing properties, for example high optical transmittance and tunable optical haze, have been found with nanocellulose paper.[15-17]

A variety of methods have been developed to confer electrical conductivity to paper. Typically, these methods involve depositing conductive materials such as carbon nanotubes (CNTs), graphene, metallic nanowires onto a paper substrate by filtration, sputtering,[18] airbrushing,[19] a variety of printing methods (inkjet printing[20], Meyer rod coating, spray coating, gravure coating[21] etc.), or soak-polymerizing conductive polymers such as polypyrrole(PPy) in paper matrix.[22, 23] Despite these substantial efforts, the sheet resistance of most current conductive papers (1-100 Ω/sq) is still much higher than metal coils (1 mΩ/sq-0.5 Ω/sq) and even ITO glass (~10 Ω/sq). To our

[a] State Key Laboratory of Pulp and Paper Engineering, South China University of Technology, Guangzhou 510640, China.
[b] Fischell Department of Bioengineering and Institute for Bioscience and Biotechnology, University of Maryland, College Park, Maryland, MD 20742, USA.
[c] Liaoning Province Key Laboratory of Pulp and Papermaking Engineering, Dalian Polytechnic University, Dalian, Dalian 116034, China.
Electronic Supplementary Information (ESI) available: [details of any supplementary information available should be included here]. See DOI: 10.1039/x0xx00000x

knowledge, the most conductive paper reported to date integrated the use of CNTs and Ag NWs and offered a sheet resistance of 1 Ω/sq.[24] These results demonstrate exciting possibilities for conducting paper, yet despite this progress there remains a need to develop inexpensive and stable fabrication methods that can complement the existing high-volume low-cost methods of conventional paper manufacturing.

Here, we report a highly conductive, pliable and foldable Cu/Cellulose paper, which was enabled by a simple, low-cost and scalable wet-processing method to coat highly conductive metal film onto common cellulose paper using an adhesion method inspired from nature. In nature, marine mussels strongly adhere onto a variety of substrates in wet environment due to the catecholic moieties (e.g. dopamine residues) in the mussel adhesive proteins.[25] The catecholic amino acid dopamine is also susceptible to self-polymerization to form polydopamine (PDA) that can strongly adhere to virtually any substrates and chelate with metal ions.[26-28] Although PDA has been intensively studied as a surface coating agent for broad applications in the past decade,[26, 29] its function in fabricating conductive nano metal film has never been found. Herein, we selected copper (Cu) because it possesses the second highest electrical conductivity ($\sigma = 5.96 \times 10^7$ S/m) among metals, it is inexpensive with a price that is only 1% that of silver, and we observed it can be electrolessly deposited onto cellulose paper that has been pre-functionalized with PDA as a functional interfacial layer. We report that our Cu/cellulose paper offers high conductivities with a sheet resistance as low as 0.01 Ω/sq as well as excellent stability due to the strong adhesion between metal and cellulose substrates. In addition, the defined nano and micro-structure of copper coating confers highly hydrophobic and self-cleaning properties, high photothermal conversion efficiency, and excellent electromagnetic interface (EMI) shielding effectiveness. We envision this high-performance paper electrode would satisfy the demand for a vast range of applications such as flexible electronics, packaging, and medical applications.

Results and discussion

In-situ growth of copper nanoparticles (NPs) on cellulose substrate

Figure 1A illustrates the fabrication approach for growing copper on a cellulose substrate (yarn, paper, or fabric). The cellulosic is first immersed in dilute dopamine aqueous solution (1 mg ml^{-1}, 10 mM Tris, pH=8.5) to assemble a thin adherent dopamine film through interactions between the catechol groups in dopamine and the exposed hydroxyl groups in cellulose paper, and the self-polymerization of dopamine under these mild alkaline conditions to produce an adherent polydopamine (PDA) coating. PDA contains both catechol and amine functional groups that can act as reducing agents and binding reagents and thus PDA has been found to be a versatile platform for secondary reactions.[30-36] In the next step, the PDA-functionalized cellulose paper is sequentially dipped

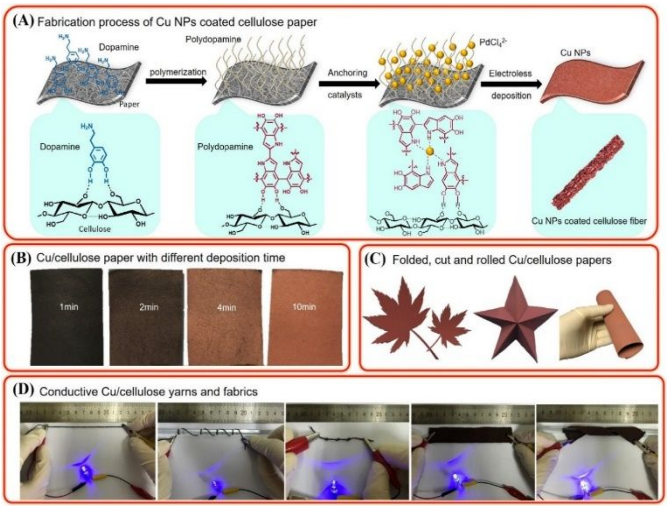

Figure 1. The in-situ growth of a Cu nanoparticle (NP) layer on cellulose substrate. (A) Scheme of the fabrication process of Cu/cellulose paper; (B) Images of Cu/cellulose paper with increasing electroless deposition (ELD) time. (C) Different Cu/cellulose paper forms obtained by cutting, folding and rolling. (D) Conductive Cu/cellulose yarns and Cu/cellulose fabrics obtained using the same method.

in the catalyst ($(NH_4)_2PdCl_4$) solution and then the $CuSO_4$ solution to initiate an electroless deposition (ELD) of copper.

This fabrication method is a completely solution-based procedure that can potentially be applied for conventional roll-to-roll processing for mass production of paper-based electronics. In this process, the PDA interfacial layer performs two key functions: confers strong adhesion to the cellulose substrate and enables catalyst chelation for subsequent ELD. ELD results in a visible color change from the dark PDA coating to the glossy metallic purple (Figure 1B). The resulting Cu/cellulose paper still retains the form of cellulose paper, and can be easily cut, folded and rolled into various shapes and structures (Figure 1C). This fabrication process is broadly applicable to cellulosics and can be extended from paper to yarn and fabric platforms. For instance, Figure 1D shows stable lighting of blue light-emitting-diodes (LED) by the Cu functionalized cellulose yarn and fabric, and these electrical properties were not destroyed by twisting, knotting, bending and twining.

The successful deposition of Cu on the paper substrate is confirmed by the X-ray diffraction (XRD) pattern of the composite (Figure 2A), with the peaks at 43.40°, 50.41°, 74.34° assigned to the diffraction planes of (111), (200), (220) of the face-centered cubic crystalline copper (JCPDS file no. 04-0836). In addition, the well-defined diffraction peaks located at 2θ=14.80°, 16.50°, 22.62°, 34.25° are assigned to the diffraction planes of (101), (10 $\bar{1}$), (200), (040), respectively, of semi-crystalline cellulose I.[37]

The Cu/cellulose paper was further examined by X-ray photoelectron spectroscopy (XPS) (Figure 2B and C), which shows evidence for the elements C, O and Cu. The peaks for O and C are assigned to cellulose, whereas the new peaks for Cu 2p results from the generation of Cu crystals. The Cu 2p spectra of the Cu/cellulose paper consisted of two individual peaks at~933.8 and ~932.2 eV attributed to CuO and Cu_2O binding energies, respectively, suggesting the surface of Cu

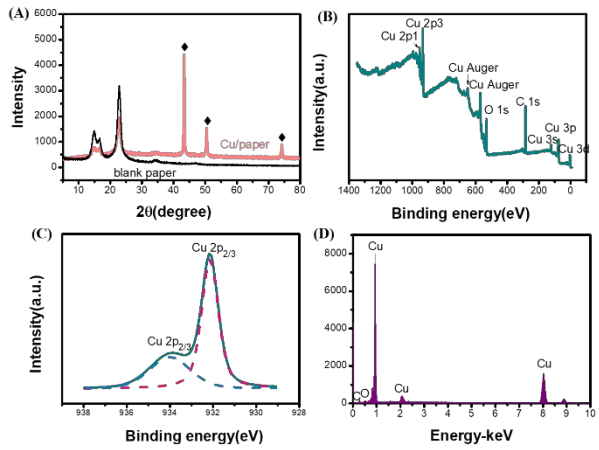

Figure 2. Chemical characterization of Cu/cellulose. (A) X-Ray diffraction (XRD) patterns of the blank paper and Cu/cellulose paper. (B) Wide scan X-ray photoelectron spectroscopy (XPS) spectra and (C) high-resolution XPS spectra of Cu 2p of Cu coated papers. (D) Energy dispersive X-ray spectroscopy (EDS) spectrum of the Cu coated filter paper.

nanoparticle was susceptible to oxidation, mainly forming a composite structure of Cu–Cu_2O.[38, 39] Finally, energy dispersive X-ray spectroscopy (EDS) analysis (Figure 2D) also quantitatively confirmed the Cu feature on the cellulose fibers.

The morphology of the Cu paper after 20 minutes ELD is shown in Figure 3(A-C). The first observation is that the Cu is organized onto cellulose as nanoparticles (NPs) that uniformly coat the cellulose fibers, and the morphology of blank paper can be seen in Fig S1. The SEM image in Figure 3 indicates a binary structure (micro-and nanostructure) on the surface of the cellulose fiber. Specifically, on the surface, papillae with average diameter of about 5 μm can be seen (yellow circles labelled in Figure 3C) and the size of the papillae increased from dozens of nanometers to several micrometers with ELD time increased from 5min to 30min (Supporting Information Figure S2). Numerous sub-nm pins were observed to be distributed on papillae, and they were uniformly coated on the cellulose fiber when the papillae became dense (Figure 3B). The uniform distribution of papillae on the surface ensure that the surface contact area available for water is very small while the hydrophobic nano-pins prevent the penetration of water, and this results in a large water contact angle (about 143°).[40, 41] According to previous researches, the polymerization process and the structure of polydopamine is complicated, and the interactions of polydopamine is complicated due to the covalent bonds between the aryl rings of the monomers, intra and interchain noncovalent interactions including hydrogen bonding, π-stacking and charge transfer[42-46]. The complicated structure of polydopamine may play an important role during the nucleation and growth of copper nanoparticles, leading to the special binary structure.[47-53]

The special binary structure of the Cu NPs layer on cellulose endows the composite material with interesting highly-hydrophobic and self-cleaning properties, as illustrated in Figure 3D. This self-cleaning capability is illustrated by the dirt removal test in Figure 3(E-G) which shows a stream of water can clean dirt from the surface of Cu/cellulose paper. This

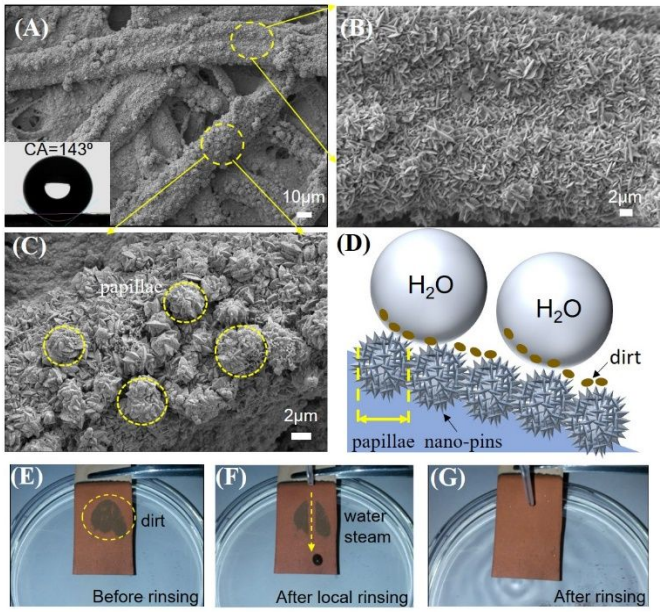

Figure 3. The copper coating shows a binary nanostructure (papillae and pin) that confer highly hydrophobic and self-cleaning properties. (A) SEM images of the Cu NPs coated filter paper with ELD time of 20 min. The insert shows the water contact angle measurement. (B-C) Partially enlarged SEM images that reveal the binary nanostructure. (D) Schematic illustration of the binary nanostructure and their self-cleaning mechanism for Cu/cellulose paper. (E-F) Self-cleaning test shows a stream of water readily removes dirt from surface (see Movies S1 and S3 in Supporting Information).

water leaves the surface without wetting and shows excellent self-cleaning capabilities (see Movie S1 in Supporting Information). The similar binary structure and property of Cu/cellulose fabric can be seen in Figure S3 and Movie S2. The fabric was removed from the water and remained fully dry without any trace of contamination again suggesting superior self-cleaning properties.

Mechanical stability and resilience of Cu/cellulose paper

The mechanical properties of the Cu/cellulose paper were investigated to ensure the metalization process does not destroy the paper's structural integrity. The decomposition pattern and thermal stability of blank paper and Cu/cellulose papers were investigated by thermogravimetric analysis (TGA; Figure 4A) and derivative thermogravimetric analysis (DTG; Figure 4B). The decomposition process in the examined temperature range could be divided into three stages. The first weight loss (< 100 °C) was attributable to desorption of moisture, the second weight loss (around 200 °C) was due to dehydration of cellulose to dehydrocellulose, and the third weight loss (around 340 °C) occurs from cellulose pyrolysis. The percentage of pyrolysis residues of blank paper and the Cu/cellulose paper at 700 °C were 12 %, 36 %, 39 % and 47 % for 0, 10, 20, and 30 min of ELD, respectively, indicating the Cu content was increased with the ELD time. Consistent with the interpretation of the TGA results is the observation that the DTG peaks occurred at the same temperature for samples prepared at different ELD times. These results indicate that the stability of the cellulose paper is not damaged by metalization.

Figure 4C presents the typical stress-strain curves for the Cu/cellulose conductive paper samples. Increases in ELD time

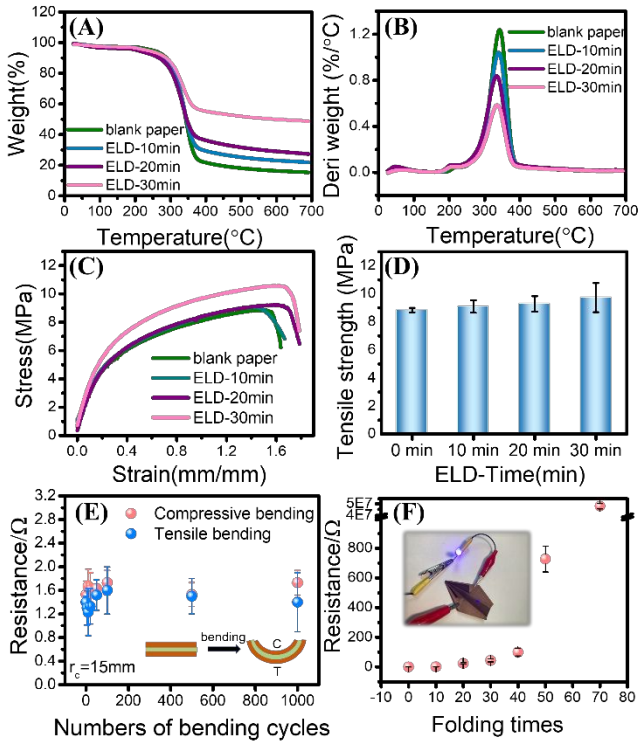

Figure 4. Structural integrity of Cu/cellulose paper. Thermal properties of the Cu/cellulose paper: (A) TGA and (B) DTG curve of the blank and Cu/cellulose papers with different ELD time. Mechanical properties of the Cu/cellulose paper: (C) Stress-strain curves and (D) tensile strength for blank paper and Cu papers with different ELD time. Pliability tests of Cu/cellulose paper: resistance changes of the Cu/cellulose paper for (E) different bending directions and (F) complex folded structures (insert picture illustrates conducting properties of folded paper).

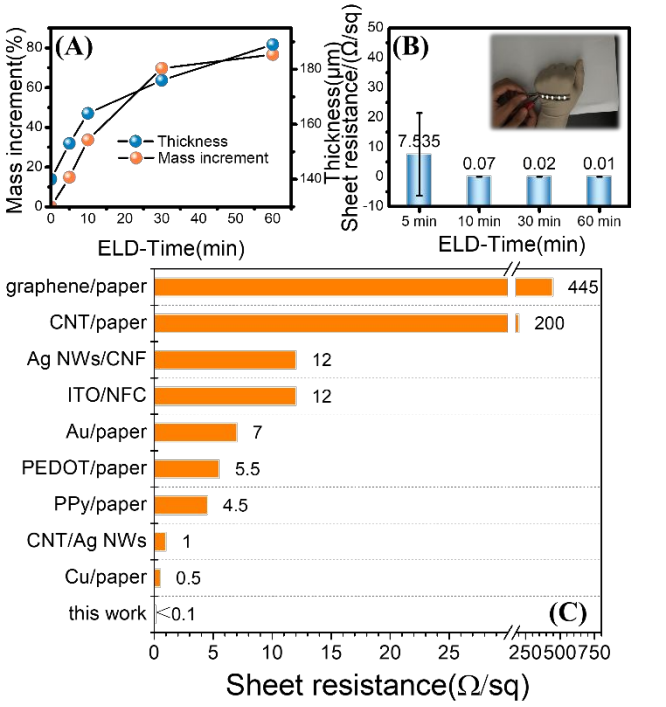

Figure 5. Electrical performance of the Cu/cellulose paper. (A) Mass and thickness increase of Cu/cellulose paper with ELD time (B) Sheet resistance decrease with ELD time (insert shows illumination of a series of LEDs by using the Cu/cellulose paper as a connecting lead). (C) Comparison of sheet resistances of conductive papers.

generally resulted in small increases in the tensile strength (Figure 4D). Similar trends were observed for the Young's modulus (Figure S4), while the elongation to break showed no obvious change with ELD time (Figure S5). These results demonstrate that the mechanical performance of the paper is retained after metalization.

Conductive stability is essential for high-speed roll-to-roll fabrication and device stability. The stability of the conducting properties imparted to the paper was evaluated by measuring sheet resistance after repeatedly deforming the Cu/cellulose paper. During bending, one face of the conductive paper is strained in tension while the other face is strained in compression stresses. And both tensile and compressive loading conditions are very important for industrial application for flexible electronics and hence different loading conditions were explored here.[54] Figure 4E illustrates that bending results in compression (C) to one face and tension (T) to the other face. Despite the strains imposed by bending, both faces retained high conductivity (low sheet resistance) even after 1000 bending cycles. Besides, the sheet resistance shows negligible changes after 1,000 cycles of bending with the bending radius as low as 5 mm, revealing that the conductivity of the Cu/cellulose paper is hardly affected by bending (see Figure S6).

As a final example illustrating the electrical stability of this flexible material, the Cu/cellulose paper was folded into a simple but compact origami structure (i.e., a paper airplane). The conductivity of this structure is illustrated by its ability to serve as a lead for a circuit that illuminates an LED bulb. To demonstrate the electrical stability, the Cu/cellulose paper was unfolded and re-folded multiple times and the resistance was measured. A small gradual increase in resistance is observed over 40 folding cycles while a larger resistance was observed after 50 times folding suggesting damage to the cellulose fibers (Figure 4F and Figure S7). Importantly, when the Cu/cellulose paper was scratched by a piece of steel, metallic luster can be observed. The scratching can't exfoliate the copper coating from the surface of the paper, and the sheet resistance kept unchanged (0.05 Ω/sq). Besides, tape adhesion test also showed the strong adhesion between Cu particles and cellulose paper(see Figure S8). These results demonstrate that the Cu/cellulose paper is flexible and the electrical properties are stable during rather extreme deformations.

Electrical performance of Cu/cellulose paper

Cellulose paper is not intrinsically conductive and has a sheet resistance of about 10^{15} Ω/sq,[22] thus conducting materials must be added to confer conductivity. Figure 5A shows that the mass and thickness of composite Cu/cellulose paper increased with increased ELD time. The assembly of Cu NPs confers conductivity to the cellulose paper reducing the sheet resistance (Rs) by 16 orders of magnitude to 0.07 Ω/sq after only 10 min of ELD (Figure 5B). Increasing ELD time to 60 minutes resulted in an extremely low Rs of around 0.01 Ω/sq (conductivity of 5×10^5 S/m). This Cu/cellulose paper with high conductivity, light weight and high strength is ideal for applications as flexible connect lead in circuits. It was demonstrated that a series of white LEDs (the lowest

operating potential is 2.5 V) can be simultaneously illuminated using the Cu paper as a connecting lead as depicted in the inset of Figure 5B.

Many researchers have reported conductive papers. ITO can be coated on cellulose paper by radio frequency (RF) magnetron sputtering, forming conductive paper with sheet resistance of 12 Ω/sq.[15] Further, some alternative conducting materials, including carbon materials, conductive polymers, metal grids, and metallic nanowires, have been extensively investigated for flexible devices.[55] Carbon materials could be attached to cellulose papers by chemical vapor deposition (CVD), Meyer rod coating or filtration.[15, 56] The sheet resistance of such materials were generally hundreds of Ω/sq.[22] In addition, low cost polymer based conductive materials (e.g., polypyrrole (PPy) and PEDOT:PSS) have also been used to confer conductivity by bar coating or polymerization *in situ*.[22] PEDOT:PSS coated paper showed very low resistance when immersed into polar solvents. To further lower the resistance, Ag NWs, Au NPs and Cu NPs have been coated onto cellulose paper by bar/spin coating, evaporated deposition or electroless deposition, and this has led to sheet resistance values as low as 0.5 Ω/sq.[24, 57-59] Figure 5C shows the sheet resistance of the Cu/cellulose paper reported here is at least one order of magnitude lower than the values previously reported conductive papers. Comparing with the other types of flexible Cu-electrodes, such as Cu/plastics and Cu foil, this Cu/cellulose paper is still competitive in conductivity, which was detailed in Table S1.[39, 59-65] Importantly, these high conductivities were achieved using solution-processing methods, that are highly controllable, low-cost, and readily scalable. Therefore, we envision the Cu/cellulose fabricated by polydopamine modification will be competitive to other conductive papers both in terms of performance (i.e., conductivity and stability) and cost.

Electromagnetic interface (EMI) shielding property of Cu/cellulose paper

The rapid development of modern electronics packed with highly integrated circuits generates severe electromagnetic radiation, which leads to harmful effects on highly sensitive precision electronics devices as well as the living environment for humans.[66, 67] Thus, there is a need for lightweight and flexible materials with excellent EMI shielding performance for applications that include portable and wearable devices.[68] The EMI shielding effectiveness (SE) of unmodified cellulose paper is nearly 0 dB due to their insulating feature.[69] When paper was coated with Cu NPs, EMI SE increases due to a combination of three effects illustrated in Figure 6A: reflection at the surface of paper due to the impedance mismatch between Cu NPs and air; absorption by Cu coated cellulose fiber resulting in the energy dissipation of electromagnetic microwave; and the multiple internal reflection between Cu coated cellulose fibers.[70] The EMI SE of the Cu/cellulose paper samples, whose conductivity are shown in Table S2, was evaluated in Figure 6B. The EMI SE of the Cu paper samples with ELD for 10 min was about 67 dB in the low frequency range of 10 MHz-1.5 GHz. Further increase ELD time resulted

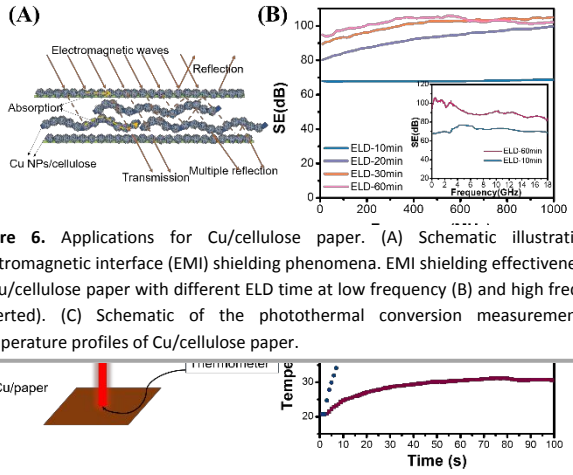

Figure 6. Applications for Cu/cellulose paper. (A) Schematic illustration of Electromagnetic interface (EMI) shielding phenomena. EMI shielding effectiveness (SE) of Cu/cellulose paper with different ELD time at low frequency (B) and high frequency (inserted). (C) Schematic of the photothermal conversion measurement. (D) Temperature profiles of Cu/cellulose paper.

in higher EMI SE of the Cu paper. Importantly, the EMI SE value of Cu paper with ELD of 60 min remained 90 dB in the high frequency of 1.5 GHz-18 GHz. This SE value is far higher than the target value of EMI SE required for practical applications (≈20 dB), indicating this highly conductive papers can be used as an effective EMI shielding material.

Photothermal conversion property of Cu/cellulose paper

Photoinduced heating of nanoparticles using near-infrared (NIR) or visible light has attracted much interest in recent years for cancer therapy, sterilization, evaporation system and other applications.[71, 72] In this work, Figure 6C showed the diagram of the photothermal conversion measurement, Cu/cellulose paper was irradiated by an 808 nm infrared diode laser, and a thermometer was used to test the real-time temperature of the paper. Excellent photothermal conversion properties were established with this Cu/cellulose paper (Figure 6D) and fabric (Figure S9). Both of the materials exhibited a sharp increase in temperature, and the temperature increase approached a plateau after about 40 s irradiation, indicating that the conductive paper and fabric could rapidly convert laser energy to environmental heat due to the electron-phonon and phonon-phonon process, which may be potentially applied in photothermal therapy, desalination, fractionation and sterilization.

Conclusions

In summary, we have successfully fabricated highly conductive paper through Cu NPs coating using a simple, low-cost and scalable solution-processing method based on polydopamine adhesion. The Cu/cellulose paper retains the intrinsic mechanical strength and pliability of paper, while achieving high electrical conductivities (Rs of 0.01 Ω/sq) and outstanding bending flexibility and stability. Moreover, the conductive paper has the excellent self-cleaning, photothermal conversion and EMI shielding properties, which could be used as wearable thermotherapy, self-cleaning or protective electronics. These results demonstrate that this low-cost and scalable fabrication method offers exciting opportunities for a range of applications in flexible and wearable electronics.

Experimental

Materials: Dopamine hydrochloride (DOPA, 98% purity) and ammonium tetrachloropalladate ($(NH_4)_2PdCl_4$) (Pd ≥36.5%) were purchased from Aladdin Chemistry Co., Ltd. Tris(hydroxymethyl)aminomethane (ACS, ＞ 99.8%) were obtained from Shanghai Yuanye Bio-Technology Co., Ltd. Copper sulfate pentahydrate ($CuSO_4•5H_2O$) (AR, 99%), Potassium sodium tartrate tetrahydrate($C_4H_4O_6KNa•4H_2O$) (ACS, 99%), Sodium hydroxide (NaOH) (AR, 96%) and formaldehyde (HCHO) (AR, 37%) were obtained from Shanghai Macklin Biochemical Co., Ltd.

Preparation of Cu/cellulose conductive papers: Filter papers or fabrics with specific size were dried at 105 °C in a vacuum oven overnight. Then the dried papers or fabrics were immersed into dopamine solution (1 mg ml^{-1}, pH=8.5, 10 mM Tris buffer) at room temperature overnight to form a polydopamine layer on the surface of the substrates, followed by washing thoroughly with deionized water. These polydopamine coated papers/fabrics were soaked in $(NH_4)_2PdCl_4$ (0.2~1 mg ml^{-1}) solution with stirring for 30 min at least, and then rinsed with DI water repeatedly. Finally, the ELD of Cu on papers/fabrics was performed with different time in a plating bath consisting of a 1:1 mixture of freshly prepared solution A and B, solution A contains NaOH (12 g/L), $CuSO_4•5H_2O$ (13 g/L), and potassium sodium tartrate (29 g/L) in DI. Solution B is a HCHO (9.5 ml/L) aqueous solution. After ELD, all the samples were washed with DI water and dried at 50 °C in the vacuum.

Characterization: X-ray photoelectron spectroscopy (XPS) results were detected on an AMICUS (Shimadzu, Japan) spectrometer with X-ray source Mg Kα, using monochromated Mg Kα radiation (1253.6 eV). The crystal structure was measured by an X-ray diffractometer (XRD, Bruker D8 Advance) equipped with a Cu Kα X-ray tube. The acquisition was performed in the range of 5 to 80 ° in θ-2θ mode with a scan angle of 0.5° and a step size of 0.02° at a scanning speed of 0.1° $step^{-1}$. The thermal stability of the composited papers was evaluated using thermogravimetric analysis (TGA Q500, TA, USA), in which samples were heated in an aluminium crucible at a rate of 10 °C min^{-1} from ambient temperature to 700 °C, continually flushed with a nitrogen flow of 25 ml/min. The tensile test was carried out using a micro tensile tester (INSTRON, 5565, USA) with a 50 mm gauge length (dimensions 15 mm × 100 mm) at a tensile velocity of 2 mm/min. The morphology of the samples was carried out with a scanning electron microscope (SEM, Hitachi, Japan) and a field-emission scanning electron microscope (FE-SEM, LEO 1530VP, Germany). The contact angle was measured by using a Ramé-Hart Model 100 Contact Angle Goniometer with a micro-syringe attachment (manual system). The resistance (R, Ω) of the samples were measured by the ohmmeter(UT52, MULTIMETER). The sheet resistance (Rs, Ω/sq) of the samples were measured by a four-probe method (RTS-8, 4 PROBE TECH, China). The corresponding volume conductivity (σ, S m^{-1}) was calculated by the formula: $\sigma = 1/(R_S t)$, where t (m) is the thickness of conductive paper. The EMI SE was measured at room temperature in the frequency range of 8-18 GHz using a WILTRON 54169A scalar measurement system. The samples were cut to rectangle with a dimension of 140 mm × 140 mm to fit the waveguide sample holder. Photothermal conversion properties were tested by an 808 nm infrared diode laser with a power density of 4 W cm^{-2} (Changchun New Industries Optoelectronics Technology Co., Ltd.) and a thermometer (UNI-T 1310, UNI-T Electronic Crop).

Conflicts of interest

There are no conflicts to declare.

Acknowledgements

This work was supported by the grants from the National Science Foundation of China (51673072) and the National Program for Support of Top-notch Young Professionals of China. Prof. G. F. Payne thanks the support of United States National Science Foundation (DMREF-1435957).

Notes and references

1. B. C. Jang, Y. Nam, B. J. Koo, J. Choi, S. G. Im, S. H. K. Park and S. Y. Choi, *Adv. Funct. Mater.*, 2018, **28**, 1704725.
2. J. Choi, Y. S. Shim, C. H. Park, H. Hwang, J. H. Kwack, D. J. Lee, Y. W. Park and B. K. Ju, *Small*, 2018, **14**, 1702567.
3. H. L. Zhu, Z. G. Xiao, D. T. Liu, Y. Y. Li, N. J. Weadock, Z. Q. Fang, J. S. Huang and L. B. Hu, *Energy Environ. Sci.*, 2013, **6**, 2105-2111.
4. X. Gao, L. Huang, B. Wang, D. Xu, J. Zhong, Z. Hu, L. Zhang and J. Zhou, *ACS Appl. Mater. Interfaces*, 2016, **8**, 35587-35592.
5. Y. H. Jung, T. H. Chang, H. L. Zhang, C. H. Yao, Q. F. Zheng, V. W. Yang, H. Y. Mi, M. Kim, S. J. Cho, D. W. Park, H. Jiang, J. Lee, Y. J. Qiu, W. D. Zhou, Z. Y. Cai, S. Q. Gong and Z. Q. Ma, *Nat. Commun.*, 2015, **6**, 7170.
6. P. Cataldi, I. S. Bayer, F. Bonaccorso, V. Pellegrini, A. Athanassiou and R. Cingolani, *Adv. Electron. Mater.*, 2015, **1**, 15000224.
7. Y. Zheng, Z. He, Y. Gao and J. Liu, *Sci. Rep.*, 2013, **3**, 1786.
8. H. Tao, L. R. Chieffo, M. A. Brenckle, S. M. Siebert, M. Liu, A. C. Strikwerda, K. Fan, D. L. Kaplan, X. Zhang and R. D. Averitt, *Adv. Mater.*, 2011, **23**, 3197-3201.
9. M. Nogi, C. Kim, T. Sugahara, T. Inui, T. Takahashi and K. Suganuma, *Appl. Phys. Lett.*, 2013, **102**, 181911.
10. Y. Q. Liu, K. He, G. Chen, W. R. Leow and X. D. Chen, *Chem. Rev.*, 2017, **117**, 12893-12941.
11. M. Nogi, S. Iwamoto, A. N. Nakagaito and H. Yano, *Adv. Mater.*, 2009, **21**, 1595-1598.
12. Q. Cheng, Z. M. Song, T. Ma, B. B. Smith, R. Tang, H. Y. Yu, H. Q. Jiang and C. K. Chan, *Nano Lett.*, 2013, **13**, 4969-4974.
13. M. Nogi, M. Karakawa, N. Komoda, H. Yagyu and T. T. Nge, *Sci. Rep.*, 2015, **5**, 17254.
14. C. H. Lin, D. S. Tsai, T. C. Wei, D. H. Lien, J. J. Ke, C. H. Su, J. Y. Sun, Y. C. Liao and J. H. He, *ACS Nano*, 2017, **11**, 10230-10235.
15. L. Hu, G. Zheng, J. Yao, N. Liu, B. Weil, M. Eskilsson, E. Karabulut, Z. Ruan, S. Fan, J. T. Bloking, M. D. McGehee, L.

Wagberg and Y. Cui, *Energy Environ. Sci.*, 2013, **6**, 513-518.
16. H. L. Zhu, Z. Q. Fang, C. Preston, Y. Y. Li and L. B. Hu, *Energy Environ. Sci.*, 2014, **7**, 269-287.
17. M. Nogi and H. Yano, *Adv. Mater.*, 2008, **20**, 1849-1852.
18. M. C. Hsieh, C. Kim, M. Nogi and K. Suganuma, *Nanoscale*, 2013, **5**, 9289-9295.
19. A. Asadpoordarvish, A. Sandstrom, C. Larsen, R. Bollstrom, M. Toivakka, R. Osterbacka and L. Edman, *Adv. Funct. Mater.*, 2015, **25**, 3238-3245.
20. L. Yang, A. Rida, R. Vyas and M. M. Tentzeris, *IEEE T. Microw. Theory*, 2007, **55**, 2894-2901.
21. A. Hubler, B. Trnovec, T. Zillger, M. Ali, N. Wetzold, M. Mingebach, A. Wagenpfahl, C. Deibel and V. Dyakonov, *Adv. Energy Mater*, 2011, **1**, 1018-1022.
22. L. Yuan, B. Yao, B. Hu, K. Huo, W. Chen and J. Zhou, *Energy Environ. Sci.*, 2013, **6**, 470-476.
23. D. D. Li, W. Y. Lai, Y. Z. Zhang and W. Huang, *Adv. Mater.*, 2018, **30**, 1704738.
24. L. B. Hu, J. W. Choi, Y. Yang, S. Jeong, F. La Mantia, L. F. Cui and Y. Cui, *Proc. Natl. Acad. Sci. U. S. A.*, 2009, **106**, 21490-21494.
25. Q. Ye, F. Zhou and W. M. Liu, *Chem. Soc. Rev.*, 2011, **40**, 4244-4258.
26. H. Lee, S. M. Dellatore, W. M. Miller and P. B. Messersmith, *Science*, 2007, **318**, 426-430.
27. C. Zhang, Y. Ou, W. X. Lei, L. S. Wan, J. Ji and Z. K. Xu, *Angew. Chem. Int. Edit.*, 2016, **55**, 3054-3057.
28. E. Filippidi, T. R. Cristiani, C. D. Eisenbach, J. H. Waite, J. N. Israelachvili, B. K. Ahn and M. T. Valentine, *Science*, 2017, **358**, 502-505.
29. K. S. Schanze, H. Lee and P. B. Messersmith, *ACS Appl. Mater. Interfaces*, 2018, **10**, 7521-7522.
30. Y. Liu, K. Ai and L. Lu, *Chem. Rev.*, 2014, **114**, 5057-5115.
31. Y. Fu, L. Liu, L. Q. Zhang and W. C. Wang, *ACS Appl. Mater. Interfaces*, 2014, **6**, 5105-5112.
32. S. Y. Ma, L. Liu, V. Bromberg and T. J. Singler, *ACS Appl. Mater. Interfaces*, 2014, **6**, 19494-19498.
33. C. A. Hong, H. Y. Son and Y. S. Nam, *Sci. Rep.*, 2018, **8**, 7738.
34. Y. Y. Song, H. J. Jiang, B. B. Wang, Y. Kong and J. Chen, *ACS Appl. Mater. Interfaces*, 2018, **10**, 1792-1801.
35. T. Akter and W. S. Kim, *ACS Appl. Mater. Interfaces*, 2012, **4**, 1855-1859.
36. Y. X. Jin, Y. R. Cheng, D. Y. Deng, C. J. Jiang, T. K. Qi, D. L. Yang and F. Xiao, *ACS Appl. Mater. Interfaces*, 2014, **6**, 1447-1453.
37. Y. Guo, X. Wang, X. Shu, Z. Shen and R.-C. Sun, *J. Agric. Food Chem.*, 2012, **60**, 3900-3908.
38. B. Q. Jia, Y. Dong, J. P. Zhou and L. N. Zhang, *J. Mater. Chem. C*, 2014, **2**, 524-529.
39. X. Q. Liu, H. X. Chang, Y. Li, W. T. S. Huck and Z. J. Zheng, *ACS Appl. Mater. Interfaces*, 2010, **2**, 529-535.
40. M. J. Liu, S. T. Wang and L. Jiang, *Nat. Rev. Mater.*, 2017, **2**, 17036.
41. M. Nordenstrom, A. V. Riazanova, M. Jarn, T. Paulraj, C. Turner, V. Strom, R. T. Olsson and A. J. Svagan, *Sci. Rep.*, 2018, **8**, 3647.
42. Y. L. Liu, K. L. Ai and L. H. Lu, *Chem. Rev.*, 2014, **114**, 5057-5115.
43. J. Liebscher, R. Mrowczynski, H. A. Scheidt, C. Filip, N. D. Hadade, R. Turcu, A. Bende and S. Beck, *Langmuir*, 2013, **29**, 10539-10548.
44. F. Bernsmann, V. Ball, F. Addiego, A. Ponche, M. Michel, J. J. D. Gracio, V. Toniazzo and D. Ruch, *Langmuir*, 2011, **27**, 2819-2825.
45. S. Hong, Y. S. Na, S. Choi, I. T. Song, W. Y. Kim and H. Lee, *Adv. Funct. Mater.*, 2012, **22**, 4711-4717.
46. N. F. Della Vecchia, R. Avolio, M. Alfe, M. E. Errico, A. Napolitano and M. d'Ischia, *Adv. Funct. Mater.*, 2013, **23**, 1331-1340.
47. J. Ryu, S. H. Ku, H. Lee and C. B. Park, *Adv. Funct. Mater.*, 2010, **20**, 2132-2139.
48. S. Kim and C. B. Park, *Biomaterials*, 2010, **31**, 6628-6634.
49. J. H. Kong, C. Y. Zhao, Y. F. Wei and X. H. Lu, *ACS Appl. Mater. Interfaces*, 2015, **7**, 24279-24287.
50. Z. Y. Li, A. Ottmann, T. Zhang, Q. Sun, H. P. Meyer, Y. Vaynzof, J. H. Xiang and R. Klingeler, *J. Mater. Chem. A*, 2017, **5**, 3987-3994.
51. L. S. Sun, C. L. Wang, X. X. Wang and L. M. Wang, *Small*, 2018, **14**.
52. J. Ryu, S. H. Ku, M. Lee and C. B. Park, *Soft Matter*, 2011, **7**, 7201-7206.
53. M. Lee, S. H. Ku, J. Ryu and C. B. Park, *J. Mater. Chem.*, 2010, **20**, 8848-8853.
54. B. Hwang, T. Kim and S. M. Han, *Extreme Mech. Lett.*, 2016, **8**, 266-272.
55. Q. Zhang, Y. Di, C. M. Huard, L. J. Guo, J. Wei and J. Guo, *J. Mater. Chem. C*, 2015, **3**, 1528-1536.
56. H. Zhu, Z. Fang, Z. Wang, J. Dai, Y. Yao, F. Shen, C. Preston, W. Wu, P. Peng, N. Jang, Q. Yu, Z. Yu and L. Hu, *ACS Nano*, 2016, **10**, 1369-1377.
57. H. Koga, M. Nogi, N. Komoda, T. T. Nge, T. Sugahara and K. Suganuma, *NPG Asia Mater.*, 2014, **6**, e93.
58. L. Y. Yuan, X. Xiao, T. P. Ding, J. W. Zhong, X. H. Zhang, Y. Shen, B. Hu, Y. H. Huang, J. Zhou and Z. L. Wang, *Angew. Chem. Int. Edit.*, 2012, **51**, 4934-4938.
59. R. S. Guo, Y. Yu, Z. Xie, X. Q. Liu, X. C. Zhou, Y. F. Gao, Z. L. Liu, F. Zhou, Y. Yang and Z. J. Zheng, *Adv. Mater.*, 2013, **25**, 3343-3350.
60. M. Hu, Q. Guo, T. Zhang, S. Zhou and J. Yang, *ACS Appl. Mater. Interfaces*, 2016, **8**, 4280-4286.
61. J. Kwon, H. Cho, H. Eom, H. Lee, Y. D. Suh, H. Moon, J. Shin, S. Hong and S. H. Ko, *ACS Appl. Mater. Interfaces*, 2016, **8**, 11575-11582.
62. X. L. Wang, H. Hu, Y. D. Shen, X. C. Zhou and Z. J. Zheng, *Adv. Mater.*, 2011, **23**, 3090-3094.
63. Z. Z. Zhao, C. Yan, Z. X. Liu, X. L. Fu, L. M. Peng, Y. F. Hu and Z. J. Zheng, *Adv. Mater.*, 2016, **28**, 10267-10274.
64. J. Kwon, H. Cho, Y. D. Suh, J. Lee, H. Lee, J. Jung, D. Kim, D. Lee, S. Hong and S. H. Ko, *Advanced Materials Technologies*, 2017, **2**, 1600222.
65. Y. Zhang, J. N. Guo, D. Xu, Y. Sun and F. Yan, *Nano Research*, 2018, **11**, 3899-3910.
66. B. Shen, W. T. Zhai and W. G. Zheng, *Adv. Funct. Mater.*, 2014, **24**, 4542-4548.
67. X. Li, Y. Li, T. T. Guan, F. C. Xu and J. Q. Sun, *ACS Appl. Mater. Interfaces*, 2018, **10**, 12042-12050.
68. N. Li, Y. Huang, F. Du, X. B. He, X. Lin, H. J. Gao, Y. F. Ma, F. F. Li, Y. S. Chen and P. C. Eklund, *Nano Lett.*, 2006, **6**, 1141-1145.

69. J. H. Chen, J. K. Xu, K. Wang, X. R. Qian and R. C. Sun, *ACS Appl. Mater. Interfaces*, 2015, **7**, 15641-15648.
70. W. L. Song, M. S. Cao, M. M. Lu, S. Bi, C. Y. Wang, J. Liu, J. Yuan and L. Z. Fan, *Carbon*, 2014, **66**, 67-76.
71. Z. B. Zha, X. L. Yue, Q. S. Ren and Z. F. Dai, *Adv. Mater.*, 2013, **25**, 777-782.
72. Y. M. Liu, S. T. Yu, R. Feng, A. Bernard, Y. Liu, Y. Zhang, H. Z. Duan, W. Shang, P. Tao, C. Y. Song and T. Deng, *Adv. Mater.*, 2015, **27**, 2768-2774.

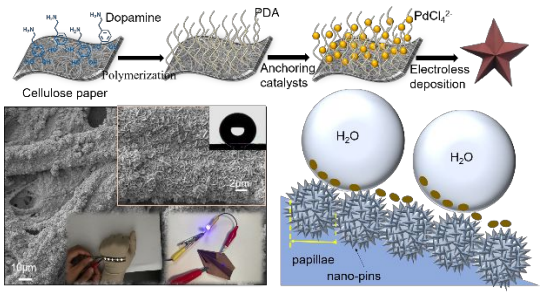

A novel and scalable approach was introduced to fabricate highly flexible and conductive paper with excellent stability and self-cleaning property.